Available online at www.sciencedirect.com

ScienceDirect

Physics Procedia 12 (2011) 141–148

Physics Procedia

LiM 2011

# Scribing of Thin-film Solar Cells with Picosecond Laser Pulses

Paulius Gečys[a]*, Gediminas Račiukaitis[a], Eimantas Miltenis[a], Alexander Braun[b], Steffen Ragnow[b]

[a] *Center for Physical Sciences and Technology, Savanoriu Ave. 231, Vilnius, LT-02300, Lithuania*
[b] *Solarion AG, Ostende 5, D-04288 Leipzig, Germany.*

**Abstract**

The thin-film CIGS technologies for photovoltaics are attractive due to their potential low cost and optimal performance. Efficiency of cells with a large area might be maintained if small segments are interconnected in series in order to reduce photocurrent in thin films and resistance losses, and laser scribing process is crucial for performance of the device. We present our results on scribing of CIGS thin-film solar cells with single and multiple parallel laser beams with the picosecond pulse duration. Solar-cell performance tests were performed before and after laser scribing together with Raman spectroscopy analysis. The quality of processing was evaluated with optical and scanning electron microscopes.

*Keywords:* Thin-film; CIGS; picosecond laser; solar cell scribing; Raman spectra; solar cell efficiency

## 1. Introduction

Continued demand for renewable energy sources stimulates development of various solar cell technologies on flexible and rigid substrates. The thin-film PV technologies based on $CuIn_xGa_{(1-x)}Se_2$ (CIGS) become more attractive due to their potential in lowering the production cost and optimization of photoelectrical performance. Other properties such as flexibility, good power-weight ratio, resistance to radiation make CIGS solar cells ideal for space use, automotive industry and complex structure building integrated applications.

CIGS has been established as the most efficient thin-film technology in converting sunlight into electricity with the theoretical limit as high as 27% [1] and a record value of 20.3% achieved in the laboratory [2]. The manufacturing costs and cell efficiency are critical factors for the wider applicability in terms of economical point of view. Efficiency of thin-film solar cells with a large active area might be maintained if small segments are interconnected in series in order to reduce photocurrent in thin films and resistance losses, and laser scribing is crucial for performance of the device.

A comprehensive study of thin film scribing for photovoltaics including CIGS with different types of lasers has been conducted by Compaan et al. [3]. Long nanosecond pulses used were found to be favorable for damage-free exposure of molybdenum in the CIGS/Mo/glass structure but excessive melt formation was observed from the CIGS layer itself. The main limiting factor to nanosecond laser processing of the multilayer $CuInSe_2$ (CIS) structures is deposition of molybdenum on walls of channels scribed in the films, and the phase transition of semiconducting

* Corresponding author. Tel.: +370-5-264-4868; Fax: +370-5-260-2317
*E-mail address*: p.gecys@ar.fi.lt


doi:10.1016/j.phpro.2011.03.116

$CuInSe_2$ to a metallic state close to the ablation area due to the thermal effect [4]. Both effects create shunts in the photo-electric device and reduce its conversion efficiency. According to the results of theoretical modeling, processing without damage is possible with ultra-short-pulse lasers [4, 5]. High power industrial picosecond lasers are available on the market and due to their high process speeds with low thermal impacts on the materials could be promising tools for CIGS solar cell scribing.

## 2. Experimental

The picosecond laser (PL10100, 10 ps, 100 kHz, from EKSPLA) was used in the ablation and scribing experiments. Experimental setup included the laser, electro-optical shutter, a nonlinear crystal for wavelength conversion, a beam expander and galvanometer scanners (ScanLab) with 80 mm focusing objectives for both 1064 nm and 532 nm wavelengths. In extension of laser scribing experiments, a diffractive optical element was used for beam splitting to realize the parallel beam scribing setup (see Fig. 1.). The lenses L1 and L2 arranged in the 4F scheme were used to control the beam separation at focal plane.

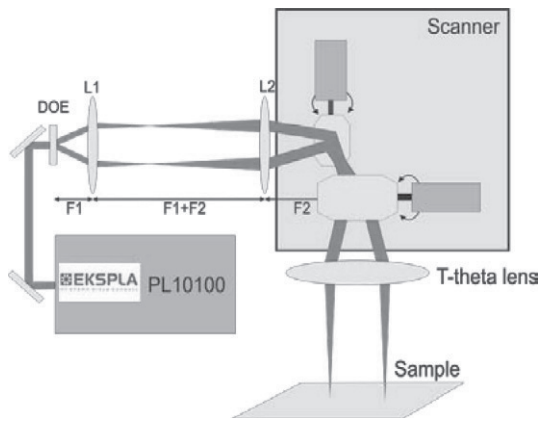


Figure. 1. Parallel beam scribing setup.

Our development was concentrated on the P3 process, scribing of the films, to expose the molybdenum back-contact by selective removal of both the top-contact and CIGS layers. Three types of complete flexible multilayer structure of the CIGS Solar cells were investigated: (i) with a thick top-contact made of ITO (1 μm), (ii) with a thick top-contact made of ZnO (350 nm), and (iii) without a top-contact. The absorber layer of $CuIn_xGa_{(1-x)}Se_2$ was 2 μm thick in all cases. A thin buffer layer of ZnO and CdS was between the top-contact and the absorber. The back-contact was made of molybdenum (1 μm) deposited on polyimide (PI) film with the thickness of 25 μm.

The quality of processing was controlled with an optical and scanning electron microscopes. Raman spectroscopy by using the confocal Raman spectrometer/microscope LabRam HR800 (Horiba Jobin Yvon) was applied to evaluate structural changes in the CIGS material after laser scribing near the ablated zone. Complete working solar cells of prefabrication stage were scribed with fundamental and second harmonics in the area between the front-contact grids, as shown in Figure 2, to evaluate alterations in solar cell performance after laser scribing. Red lines indicate separate laser scribes of 20 mm in length and the total scribe length was 360 mm. These solar cells were not final product and did not gain their optimal performance. The efficiency measurements were done at standard reference spectra AM 1.5 and 1000 $W/m^2$ total irradiance at Solarion AG, Germany. All samples were provided by Solarion AG, Germany.

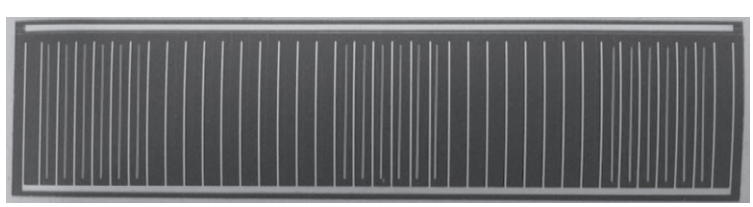

Figure. 2. Red lines indicate laser scribed trenches. The total length of the scribes was 360 mm.

## 3. Results

### *3.1. Exposure of Mo with burst of laser pulses*

Ablation with a train of laser pulses per spot was performed from the top-contact side to expose the molybdenum back-contact. Two types of experiments were realized with ablation using 2 and 10 pulses per spot with 1064 nm and 532 nm wavelengths at different laser fluences. Visual examination of craters and their size measurements were performed with optical and scanning electron microscopes. Typical SEM images of multi-pulse ablation and exposure of the Mo back-contact with different wavelengths are shown in Figure. 3.

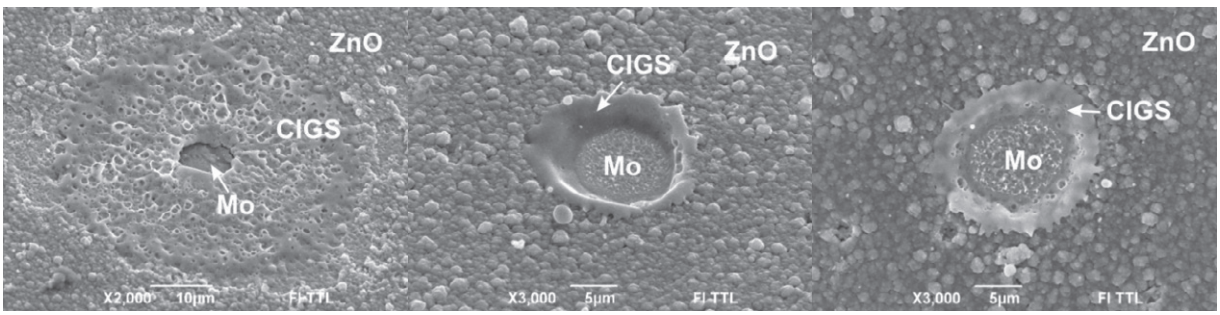


(a) (b) (c)

Figure. 3. SEM images of Mo layer exposure in ZnO(1 μm)/CIGS/Mo/Pi structure by laser pulses: (a) 44 μJ, 2 pulses@1064 nm; (b) 2 μJ, 10 pulses@1064 nm, (c) 2 μJ, 10 pulses@532 nm.

The threshold values for laser fluence required to remove the top-contact and absorber layers to expose the molybdenum film as well as the beam waist on the processed surfaces were evaluated by the method proposed by Liu [6] for Gaussian beams and are shown in Table 1. The highest thresholds to expose the Mo layer with both wavelengths were found for the structure of ITO/CdS/CIGS/Mo/PI with the thickest top-contact of 1 μm. For the structure of ZnO(350 nm)/CdS/CIGS/Mo/PI, the Mo exposure threshold values were lower due to the thinner top-contact. The lowest threshold was found for the structure without a top-contact of CdS/CIGS/Mo/PI.

Table 1. The threshold fluencies for exposure of the molybdenum back-contact and beam waist estimated from crater ablation in three types of CIGS solar cells with picosecond laser radiation at 1064 nm and 532 nm wavelengths.

| | **2 pulses** | | **10 pulses** | |
|---|---|---|---|---|
| 1064 nm | Mo exposure threshold, J/cm$^2$ | Beam waist, μm | Mo exposure threshold, J/cm$^2$ | Beam waist, μm |
| ITO(1 μm)/CdS/CIGS/Mo/PI | - | - | 1.3 | 6.3 |
| CdS/CIGS/Mo/PI | - | - | 0.84 | 7.8 |
| ZnO(350 nm)/CdS/CIGS/Mo/PI | - | - | 0.94 | 6.5 |
| 532 nm | | | | |
| ITO(1 μm)/CdS/CIGS/Mo/PI | 19.4 | 8.9 | 1.3 | 7.1 |
| CdS/CdS/CIGS/Mo/PI | 4.7 | 7.4 | 0.8 | 5.9 |
| ZnO(350 nm)/CdS/CIGS/Mo/PI | 16.7 | 7.7 | 1.05 | 6.1 |

The relationship between the exposed area of the Mo layer and the accumulated irradiation dose for 2 and 10 pulses for both wavelengths is shown in Figure. 4. The irradiation doses required to open the Mo back-contact at 1064 nm and 532 nm wavelengths were found to be similar for same structures of CIGS solar cells, although the ablation quality was different. A larger melted area of the CIGS layer was spotted at the edges of the crater when

ablating with low energy laser pulses at 532 nm wavelength, although melted CIGS was observed with both 1064 nm and 532 nm wavelengths.

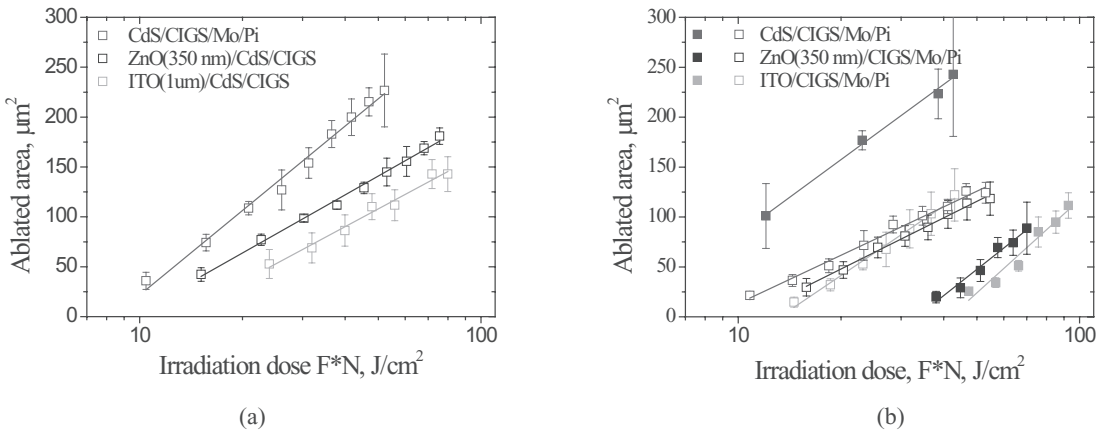


Figure. 4. Relationship between the exposed area of Mo layer and the accumulated irradiation dose for 2 (*solid dots*) and 10 (*open dots*) pulses at: (a) 1064 nm wavelength, (b) 532 nm wavelength.

At both wavelengths, the high energy laser pulses peeled the top-contact leaving extensive melt of the CIGS. While ablating CIGS material with a burst of low energy pulses, the melted area was significantly reduced. For the real scribing process, it means that lasers with a high repetition rate should be applied and the laser pulse energy could be focused to an elliptical spot [7] or split into a few channels to increase the overall process speed.

### *3.2. Scribing of CIGS to expose the Mo back-contact*

Three different types of solar cell material were laser scribed to open the Mo back-contact. The laser spot overlap along a scanning line was controlled by the translation speed at a constant pulse repetition rate. Single and multi-pass scribing methods were applied in the experiments. Various combinations of pulse energy, beam overlap and wavelength were used for selective ablation of the films. Optimal regimes for laser processing of every layer were estimated depending on the wavelength. Typical SEM images of laser scribed trenches are shown in Figure. 5.

For both wavelengths, the use of high laser pulse energy with the low pulse overlap caused poor layer removal selectivity and extensive melt formation at the edges of the scribing zone. Lowering the pulse energy and applying higher pulse overlap facilitated an increase in selectivity of layer ablation and significantly reduced melt formation in CIGS layer. With both 1064 nm and 532 nm wavelengths, smooth trenches were scribed in all three types of solar cell material with a low laser power, high pulse overlap and single pass beam scanning to open the molybdenum back-contact. Narrow melt areas were spotted at the edges of the scribe, although ablation with 1064 nm showed smoother scribe edges (Figure. 5). In both cases the back-contact was left damage-free with no Mo melt deposition on to the side walls of the laser scribed trench avoiding shunt formation.

Use of gentle ablation with a low laser power and high pulse overlap together with multi-pass scanning allowed us to achieve very smooth laser scribes with high layer selectivity, although process productivity was low. Closer view of P3 type laser scribe with infrared irradiation in ITO/CdS/CIGS/Mo/PI structure is shown in Figure. 6. The absorber layer together with thick front-contact of ITO and CdS buffer layer were completely removed to open the molybdenum back-contact. A narrow melt area of the CIGS layer was spotted at the ablated channel sidewall, although sharp separate layer interfaces without debris of melted Mo were clearly visible indicating low thermal impact of the picosecond laser pulses on the surrounding solar cell material.

In all cases with both 1064 nm and 532 nm wavelengths the melt formation at the edges of the scribe was not avoided completely due to Gaussian distribution of the laser beam and producing clean edges required the use of a flat-top shaped beam [8].

In most cases scribing with second harmonics required 20% less of laser power compared to the fundamental, although considering wavelength conversion losses and slightly lower scribing quality at 532 nm wavelength, scribing with fundamental harmonics may be more reasonable due to higher process productivity and lower cost of the scribing device.

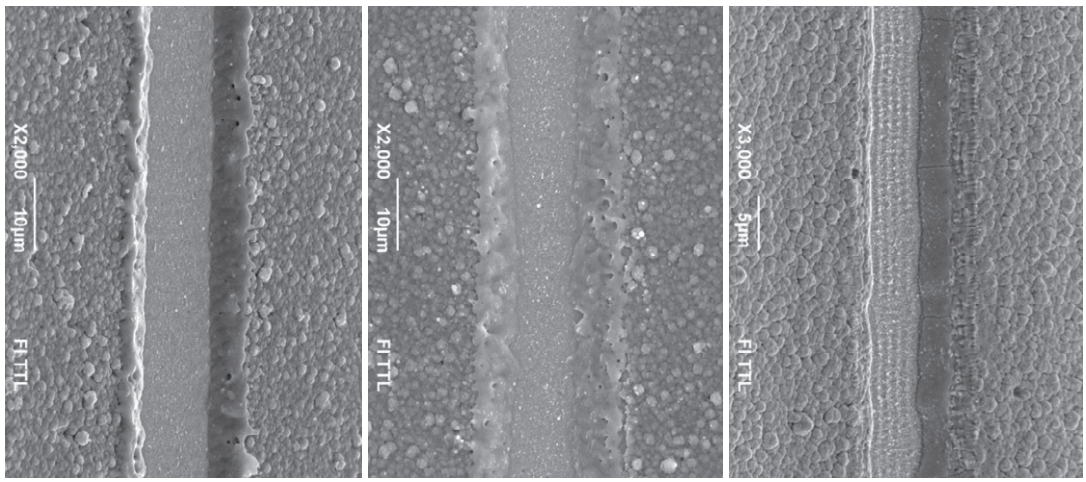


(a) (b) (c)

Figure. 5. Tilted SEM images of the P3 scribe: (a) ZnO(1 μm)/CIGS/Mo/PI structure 200 mm/s single pass@1064 nm, (b) ZnO(1 μm)/CIGS/Mo/PI structure 200 mm/s single pass@532 nm, (c) ITO(1 μm)/CdS/CIGS/Mo/PI structure 100 mm/s 2 scans@1064 nm.

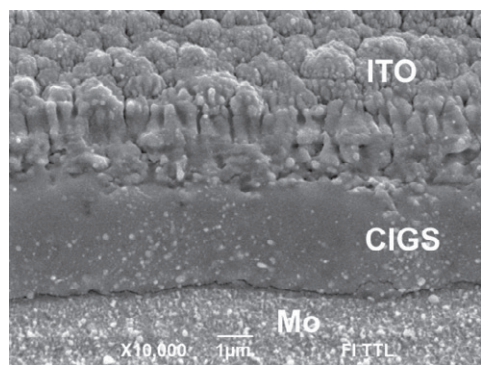


Figure. 6. Closer view of P3 type laser scribe in ITO/CdS/CIGS/Mo/PI material, 100 mm/s, 2 scans@1064 nm.

### *3.3. Raman measurements*

CIGS is thermally sensitive material and laser scribing can lead to structural changes on the melted edges of the scribe. Formation of metallic phase in the CIGS material close to the laser scribed zone may cause an internal shunt formation and reduction in solar cell performance [9]. Therefore, laser scribed areas were investigated with Raman spectroscopy to track $Cu_xSe$ secondary metallic phase formation near the scribing zone. Unwanted secondary metallic phase line $CuSe_x$ shows a peak at 262cm$^{-1}$ in Raman spectra [9]. The Raman spectrum was measured in four areas starting from the edge of the scribe as shown by the numbers in Figure. 7. For both 1064 nm and 532 nm wavelengths, Raman spectroscopy was not able to detect any $Cu_xSe$ metallic phase formation in measured areas. These measurements confirmed ability of picosecond lasers to scribe CICS thin-film solar cells with low thermally-induced structural changes of the material near the scribing zone.

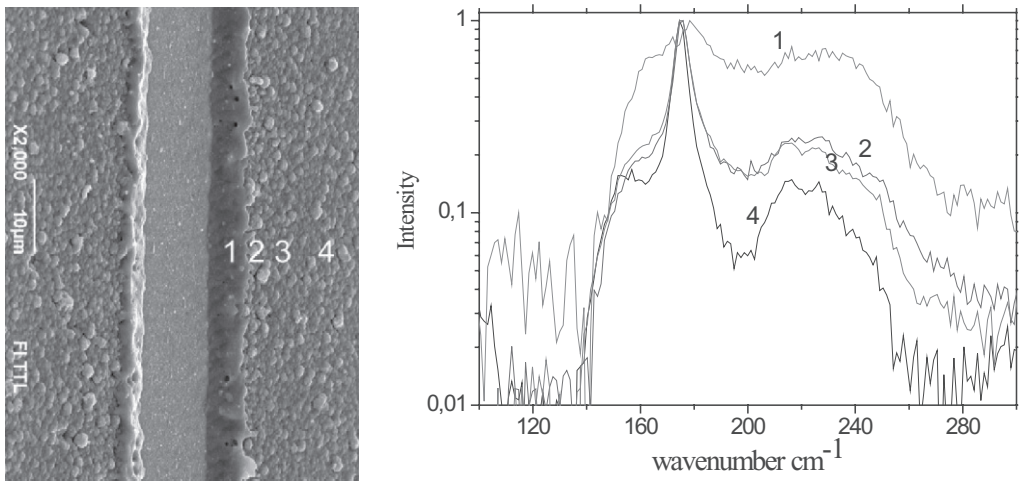


Figure. 7. Raman spectra of ZnO(1 μm)/CdS/CIGS/Mo/Pi structure. Numbers of curves correspond to a position on a sample (left).

### *3.4. Solar cell efficiency testing after laser scribing*

Complete working solar cells of prefabrication stage with the average efficiency of 10.7% and the active surface area of 32 $cm^2$ were scribed using optimal single and multi-pass scribing parameters. The total length of laser scribes was 360 mm in all cases. The efficiency tests were done before and after laser scribing to evaluate the scribe influence on the solar cell performance at the standard testing conditions (standard reference spectra AM 1.5 and 1000 $W/m^2$ total irradiance). Three solar cells were scribed with 1064 nm wavelength and two cells were processed with 532 nm wavelength. Efficiency tests after laser scribing showed an insignificant degrease in solar cell performance at both wavelengths. We used a definition of an absolute average drop of solar cell initial efficiency which is equal to the difference of efficiency before and after laser scribing process including spontaneous efficiency degradation of solar cells in time due to contact with ambient air.

Table 2. Cell efficiency test results before and after laser scribing was applied.

| Cell Nr. | Mode | Cell eff. before laser scribing, % | Cell eff. after laser scribing, % | Absolute eff. drop, % |
|---|---|---|---|---|
| 1064 nm | | | | |
| 1 | Single pass | 11,18 | 9,71 | 0,58 |
| 2 | Single pass | 10,59 | 9,60 | 0,11 |
| 3 | Multi pass | 10,08 | 9,07 | 0,13 |
| | | | Average, % | ~0.3 |
| 532 nm | | | | |
| 4 | Single pass | 11,51 | 9,86 | 0,76 |
| 5 | Multi pass | 10,71 | 9,55 | 0,28 |
| | | | Average, % | ~0.5 |

The absolute average drop of the initial solar cell efficiency was 0.3% at 1064 nm wavelength and 0.5% at 532 nm. Laser scribing induced narrow melt areas at the edges of the scribe and, most likely, generation of internal shunts provoked an insignificant reduction in the solar cell performance in these zones. The melted scribe edge area was larger when ablating with laser pulses of 532 nm wavelength and it corresponded to the higher efficiency drop compared to the 1064 nm wavelength although the defect generation with a laser at the edge of the scribe is more

statistical process and it requires a larger amount of solar cells to be tested for determining the influence of laser scribing on the solar cell performance.

### *3.5. Parallel beam scribing CIGS*

The industrial scribing applications demand cost effective high speed processes that could be easily integrated into existing production lines. To reach productive process and fit the demands from industry, the parallel beam scribing should be used in most applications. We realized the four-parallel-beams scribing of CIGS thin-film solar cells by installing a beam splitter into our experimental setup and still working with a single scanner head. The overall power required for the scribing was much lower than the maximum power of the used laser and four or more parallel beams processing could be easily realized. The distance between focused parallel laser beams was controlled by controlling the splitting angle which could be changed by applying a different beam expander in the optical setup. All laser scribing regimes fitted well in a new four-beam scribing setup, although the laser power had to be multiplied as we were working with two beams. We demonstrate that same scribing conditions (focusing, power) could be maintained for parallel beams with a proper repeatability of laser scribed trenches. This shows a potential for optimizing laser scribing processes for CIGS solar cells and fitting the demand from industry in terms of process productivity and economical point of view.

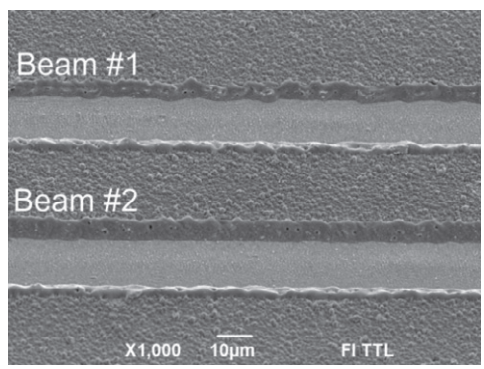


Figure. 8. SEM images of two parallel beam P3 step scribing in ZnO(1 µm)/CIGS/Mo/PI structure.

## 4. Conclusions

At both wavelengths high energy pulses peeled the top-contact leaving extensive melt of the CIGS. While ablating CIGS material with a burst of low energy pulses the melt area was significantly reduced. The irradiation doses required to expose Mo back-contact were found similar for both 1064 nm and 532 nm wavelengths, although laser pulses with the 1064 nm wavelength caused less melt formation at the edges.

Fine quality trenches were laser scribed with both wavelengths enabling us to open the Mo back-contact. Raman spectroscopy did not detect any secondary phase formation near the scribing zone, although cell efficiency tests revealed a marginal 0.3-0.5% degrease in solar cell performance for both wavelengths. The average drop of cell efficiency was 0.2% lower for 1064 nm wavelength and this may be explained by smother ablation of the CIGS by infrared radiation.

Picosecond lasers with fundamental harmonics and high repetition rates can be used in combination with a parallel beam scribing method to accomplish efficient and fast scribing process which is able to fit the demands for industrial solar cell scribing applications.

## Acknowledgements

This research was funded by a grant (No. AUT-06/2010) from the Research Council of Lithuania. We express our thanks to K. Zimmer, M. Ehrhardt, A. Wehrmann form the Leibniz institute for surface modification, Germany, for support with solar cell efficiency measurements.

## References

[1] Cheyney, T.: Thin-film CIGS starts to come of age. In: Photovolt. Int., 1 (2008), pp. 86
[2] Kho, J.: What's Behind Record-Breaking Solar Cell Efficiencies, In: Photovoltaics World, 6 (2010), pp. 24-27
[3] Compaan, A.D.; Matulionis, I.; Nakade, S.: Laser scribing of polycrystalline thin films. In: Opt. Laser Eng., 34 (2000), pp. 15
[4] Hermann, J.; Benfarah, M.; Bruneau, S.; Axente, E.; Coustillier, G.; Itina, T.; Guillemoles, J.-F.; Alloncle, P.: Comparative investigation of solar cell thin film processing using nanosecond and femtosecond lasers. In: J. Phys., D 39 (2006), pp. 453
[5] Hermann, J.; Benfarah, M.; Coustillier, G.; Bruneau, S.; Axente, E.; Guillemoles, J.-F.; Sentis, M.; Alloncle, P.; Itina, T.: Selective ablation of thin films with short and ultrashort laser pulses. In: Appl. Surf. Sci., 252 (2006), pp. 4814
[6] Liu, J.M.: Simple technique for measurements of pulsed Gaussian-beam spot sizes. In: Opt. Lett., 7 (1982), pp. 196
[7] Huber, H.P.; Englmaier, M.; Hellwig, C.; Heiss, A.; Kuznicki, T.; Kemnitzer, M.; Vogt, H.; Brenning, R.; Palm, J.: High speed structuring of CIS thin-film solar cells with picosecond laser ablation. In: Proc. SPIE, 7203 (2009), pp. 72030R
[8] Gecys, P.; Raciukaitis, G.; Ehrhardt, M.; Zimmer, K.; Gedvilas, M.: ps-laser scribing of CIGS films at different wavelengths, In: Appl. Phys. A, 101 (2010), pp. 373-378
[9] Miyazaki, H.; Mikami, R.; Yamada, A.; Konagai, M.: Cu(InGa)$Se_2$ thin film absorber with high Ga contents and its application to the solar cells, In: J. Phys. Chem. Sol., 64 (2003), pp. 2055-2058